Turkish Computational and Theoretical Chemistry

Turkish Comp Theo Chem (TC&TC)

Volume(Issue): 9(2) – Year: 2025 – Pages: 111-124

e-ISSN: 2602-3237

https://doi.org/10.33435/tcandtc.1527511

Received: 03.08.2024 ***Accepted***: 18.09.2024 *Research Article*

In Silico Assessment of the Insecticidal and Herbicidal Potential of Silichristin Isolated from Silybum Marianum: Pharmacokinetic-Toxicity properties, Molecular Docking, and Molecular Dynamics

Regadia Aissaoui[a], Med Nadjib Rebizi[a], Khadidja Boussaid[b], Elhafnaoui Lanez[c], Touhami, Lanez[c,1],

[a]Department of Chemistry, University of Djelfa, 17000, Djelfa, Algeria
[b]Research Center Agro-Pastoralism (CRAPast), 17000, Djelfa, Algeria
[c]VTRS Laboratory, University of El Oued, B.P.789, 39000, El Oued, Algeria

Abstract: The present study aims to evaluate the pesticidal potential of a series of novel silichristin analogues isolated from silybum marianum using *in silico* approaches, focusing on their effects on the 4-hydroxyphenylpyruvate dioxygenase (HPPD) and acetylcholinesterase (AChE) receptors. A combinatorial library of 729 silichristin derivatives was constructed and virtual screening was performed to evaluate their pharmacokinetic and toxicity properties. Molecular docking analyses were performed to assess the binding affinity of the most potent candidates with target proteins. Our findings revealed that all selected compounds exhibited activity against both HPPD and AChE, with SIL3 and SIL7 demonstrating the lowest binding free energies (-8.4 and -7.9 kcal/mol, respectively). Further investigation via molecular dynamic simulation indicated that SIL3 and SIL7remained stable within the HPPD and AChE active sites, with RMSD values consistently below 2Å throughout the simulation. Overall, these results suggest that the newly identified silichristin derivatives hold promise as anti-pesticide agents.

Keywords: 4-hydroxyphenylpyruvate dioxygenase (HPPD), acetylcholinesterase (AChE), virtual screening, binding affinity, RMSD.

1. Introduction

Silybum marianum, commonly known as milk thistle, is a flowering plant native to the Mediterranean region but now found in many parts of the world. It belongs to the Asteraceae family and is characterized by its distinctive spiky leaves and purple flowers. The plant has a long history of use in traditional medicine, particularly for its purported liver-protective properties [1–4]. In addition to its hepatoprotective effects, milk thistle has also been studied for its potential benefits in managing other health conditions, such as diabetes [5,6], high cholesterol [7], and certain types of cancer [8]. *Silybum marianum* has been also studied for its potential applications in agriculture, particularly in the context of herbicides and insecticides [9,10]. The active constituents of *Silybum marianum* include silymarin, which is a complex of flavonolignans, including among others silichristin extracted primarily from the seeds, wherein it is present in a higher concentration than other parts of the plant and has shown promise pesticidal applications [11,12]. However, more research is needed to fully understand the efficacy and safety of *Silybum marianum* as herbicides and insecticides.

4-hydroxyphenylpyruvate dioxygenase (HPPD) is an enzyme found in both plants and animals, including insects and pets. In insects, HPPD plays a crucial role in the biosynthesis of essential aromatic amino acids, such as tyrosine and phenylalanine, which are vital for growth, development, and survival [13,14]. In agricultural contexts, HPPD inhibitors are a class of herbicides commonly used to control weeds by interfering with the activity of HPPD in plants [14]. These

[1] Corresponding Authors
e-mail: m.zakarianejad@yahoo.com & mzakarianejad@pnu.ac.ir

inhibitors disrupt the synthesis of essential amino acids in targeted plants, leading to their death. However, they do not typically affect animals, including insects and pets, as the metabolic pathways involving HPPD in animals differ from those in plants. Recently concerns have been raised about potential indirect effects of HPPD inhibitors on non-target organisms. For example, in agricultural settings, the use of HPPD inhibitors may lead to changes in plant composition and availability of food sources for insects, potentially impacting insect populations and ecological interactions.

Acetylcholinesterase (AChE) plays a crucial role in insects, it regulates cholinergic neurotransmission, which is vital for proper functioning of the insect nervous system [15]. Specifically, AChE catalyzes the hydrolysis of the neurotransmitter acetylcholine into choline and acetate at cholinergic synapses[16,17]. This enzymatic action is necessary to terminate the signal transmission at these synapses, allowing for precise control over insect behavior and physiology. However, the significance of AChE in insects goes beyond normal neurotransmission. AChE is also the primary target of many insecticides, these insecticides work by inhibiting AChE activity, leading to the accumulation of acetylcholine at synaptic junctions [18,19]. The excessive stimulation of cholinergic receptors disrupts normal nerve function, ultimately resulting in paralysis and death of the insect.

The development of HPPD and AChE inhibitors as herbicides and insecticides respectively has been a significant area of research in pest control due to their effectiveness against a wide range of herb and insect species [20,21]. However, their non-selective action can also pose risks to non-target organisms and the environment [22].

The pesticidal potential of silichristin has gained interest due to the growing demand for sustainable pest control solutions. Traditional chemical pesticides pose environmental and health risks, prompting the search for safer alternatives. Harnessing the natural compounds present in plants like *Silybum marianum* offers a promising avenue for developing effective and eco-friendly pesticides.

In this context, our study contributes to the ongoing efforts in the field of pesticide research by identifying novel candidates derived from natural sources. By harnessing the bioactive compounds present in plants like *Silybum marianum*, we can develop sustainable and eco-friendly solutions for pest management, addressing the global challenge of pesticide resistance and environmental pollution. The present study aims to assess the suitability of silichristin analogues as herbicides and insecticides through a comprehensive in silico analysis. We constructed a combinatorial library of 729 silichristin analogues and subjected them to virtual screening to evaluate their pharmacokinetic and toxicity properties. Molecular docking analyses were then performed to investigate their binding affinity with target receptors, focusing on 4-hydroxyphenylpyruvate dioxygenase (HPPD) and acetylcholinesterase (AChE) receptors, key targets for herbicides and insecticides action. Additionally, molecular dynamics simulations were employed to study the stability and dynamics of the protein-ligand complexes.

Our study addresses the urgent need for innovative and sustainable pest management strategies by exploring the potential of silichristin analogues as novel herbicides and insecticides. Through advanced computational techniques, we aim to identify promising candidates for further experimental validation, ultimately contributing to the development of safer and more effective herb and insect control agents [23–25].

2. Computational Method

2.1. Combinatorial library

We conducted a virtual screening to generate a combinatorial library of silichristin analogues using SmiLib v2.0 software [26]. A silichristin structure served as the scaffold, with functional groups (F, OCH_3, and CH_3) utilized as building blocks alongside empty linkers. Following enumeration, we generated a total of 729 combinations of silichristin molecules. To filter these molecules based on their pharmacokinetic and toxicity properties, screening tools including SwissADME [27] and pkCSM [28] were employed. Pharmacokinetic properties were evaluated for all generated silichristin molecules within the human context, encompassing aqueous solubility, blood-brain barrier (BBB) permeability, CYP binding, and intestinal absorption.

2.2. Screening for pharmacokinetics-toxicity

We utilized the online tool SwissADME [27], provided by the Swiss Institute of Bioinformatics), to predict the pharmacokinetics proprieties for the generated silichristin analogues. The objective of this analysis was to determine whether the compounds acted as inhibitors of isoforms of the Cytochrome P450 (CYP) family. Additionally, we evaluated the pharmacokinetics regarding gastrointestinal absorption, P-glycoprotein activity, and blood-brain barrier penetration. We also used the pkCSM webserver [28] to predict the acute oral toxicity in rats LD_{50} of silichristin and all generated analogues. To select the candidate molecules from the combinatorial library, we prioritized properties critical for assessing their potential impact on human health. Specifically, we focused on the acute oral toxicity in rats.

2.3. Structural Optimization

The initial step involved optimizing the geometries of the selected silichristin analogues using molecular mechanics. Subsequently, a comprehensive re-optimization was conducted utilizing the DFT/B3LYP method with the 6-311G++(d,p) basis set, employing the Gaussian 16W program package [29]. Furthermore, the 3D structure of the reference natural pesticide silichristin was retrieved from PubChem (https://pubchem.ncbi.nlm.nih.gov/) [30].

2.4. Protein selection

Crystallized three-dimensional structures of 4-hydroxyphenylpyruvate dioxygenase (HPPD) and acetylcholinesterase (AChE) receptors were selected as foundational templates for conducting molecular docking. These structures, with PDB codes 6J63 [31] and 6xyu [32] respectively, were sourced from the Protein Data Bank [33].

2.5. Molecular docking

Molecular docking simulations were performed using the Schrödinger Maestro software [34]. Initially, the crystallized 3D protein structures were visualized using the Maestro interface and prepared using the Protein Preparation Wizard at a pH of 7. During this preparation step, water molecules and any interfering ligands were meticulously removed from the protein structures. Subsequently, the Receptor Grid was established to delineate the interaction region between the protein and the ligand. This was accomplished using the Receptor Grid Generation tool in Maestro, defining the area around the active site with coordinates (x, y, z). The number of grid points along the x, y, and z dimensions was set at 10×10×10 for both receptors, corresponding to the x, y, and z axes, respectively. Docking analysis was conducted using the Glide tool within Maestro [35]. The prepared ligands were flexibly docked into the active site of the target proteins using the Glide SP module, followed by extra precision docking with refined ligand sampling. Before docking the silichristin ligands, docking analysis was initially performed on the co-crystallized ligand to assess its binding affinity at the target protein's active site. The Ligand Interaction tool was employed to visualize the interaction diagrams of the ligands with the residues at the active site of the target protein. The number of grid points along the x, y, and z dimensions was set respectively at x = 33.05, y = 67.37, and z = 9,81.

2.6. Molecular dynamics

Molecular Dynamics (MD) simulations were used to assess the stability of protein-ligand complexes under physiological conditions. In this investigation, MD simulations with a duration 100 ns were performed on the protein-ligand complexes to analyze the behavior of the candidate ligand molecule within the binding sites of HPPD and AChE enzymes. Throughout the MD simulations, various parameters such as Root Mean Square Deviation (RMSD), Root Mean Square Fluctuation (RMSF), and radius of gyration were monitored from the trajectory data. These parameters served as critical metrics for evaluating the stability and binding affinity of the protein-ligand complexes in dynamic environments

3. Results and discussion

3.1. Virtual screening

In this study, the scaffold structure presented on Figure 1 was used to generate silichristin analogues using the functional groups (F, OCH_3, and CH_3) as building blocks alongside empty linkers. A compound library containing 729 silichristin analogues was generated.

All generated molecules underwent a rigorous virtual screening process to evaluate their potential

suitability as herbicides and insecticides. This screening involved a comprehensive assessment of toxicity properties using the pkCSM webserver. Only molecules exhibiting lower acute oral toxicity in rats compared to silichristin were selected for further analysis of their pharmacokinetic properties. Molecules failing to meet this toxicity criterion were excluded from further study. Subsequently, the selected molecules underwent additional evaluation using the SwissADME webserver to predict key pharmacokinetic parameters. Based on the data obtained from these in silico pharmacokinetic-toxicity screening models, molecules demonstrating the highest potential as candidates for herb and insect control were identified (see Table 1).

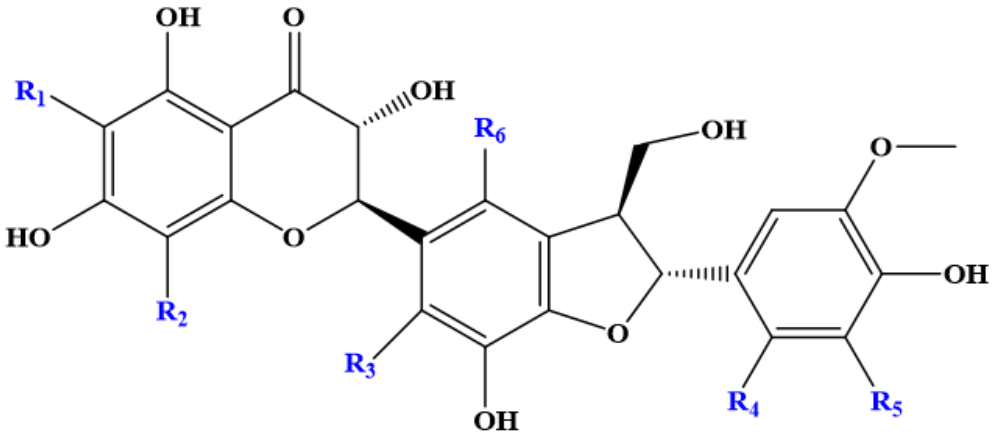

Figure.1. Scaffold structure used for the enumeration of silichristin analogues

Table 1. Selected silichristin analogues

Entry	Code	R1	R2	R3	R4	R5	R6
1	SIL1	OCH_3	OCH_3	CH_3	OCH_3	CH_3	F
2	SIL2	OCH_3	OCH_3	F	OCH_3	CH_3	OCH_3
3	SIL3	F	OCH_3	OCH_3	CH_3	F	F
4	SIL4	OCH_3	OCH_3	CH_3	CH_3	OCH_3	F
5	SIL5	F	OCH_3	OCH_3	CH_3	F	OCH_3
6	SIL6	OCH_3	OCH_3	OCH_3	F	OCH_3	F
7	SIL7	OCH_3	F	F	OCH_3	F	CH_3
8	SIL8	OCH_3	CH_3	F	F	OCH_3	F
9	SIL9	OCH_3	CH_3	F	OCH_3	OCH_3	OCH_3
10	SIL10	OCH_3	OCH_3	F	F	OCH_3	CH_3
11	SIL11	OCH_3	CH_3	F	OCH_3	CH_3	OCH_3
12	SIL12	OCH_3	OCH_3	OCH_3	OCH_3	OCH_3	F
13	SIL13	OCH_3	OCH_3	F	OCH_3	F	CH_3
14	SIL14	OCH_3	OCH_3	CH_3	OCH_3	F	CH_3
15	SIL15	OCH_3	OCH_3	F	OCH_3	OCH_3	OCH_3
16	SIL16	OCH_3	F	OCH_3	OCH_3	F	CH_3
17	SIL17	OCH_3	OCH_3	F	F	OCH_3	F
18	SIL18	OCH_3	OCH_3	OCH_3	OCH_3	F	OCH_3
19	SIL19	OCH_3	OCH_3	CH_3	OCH_3	CH_3	OCH_3
20	SIL20	OCH_3	OCH_3	F	F	F	CH_3

The tabulated data presented in Table 2 provides a comprehensive overview of the pharmacokinetic and toxicity profiles obtained for the selected analogues of silichristin derived through our investigation. These properties include LogKp (skin permeation), CYP enzyme inhibition, P-glycoprotein (P-gp) substrate status, blood-brain barrier (BBB) permeability, and gastrointestinal (GI) absorption.

Silichristin and its analogues exhibit a range of LogKp values, indicative of their skin permeation potential. From the pharmacokinetic insights provided in Table 2, it was determined that all compounds exhibited low skin permeability. Sil12 and Sil18 stand out with particularly more negative Log Kp values, suggesting limited skin permeation potential.

Regarding CYP enzyme inhibition, none of the compounds demonstrate inhibitory effects on CYP enzymes, indicating potential safety in terms of compound metabolism. Also, none of the compounds are predicted to be P-gp substrates, which may influence their distribution and elimination from the body. Regarding BBB permeability, none of the compound is predicted to permeate the BBB. All analogues exhibit low GI absorption, suggesting limited absorption in the gastrointestinal tract.

Table 2. Evaluation of Pharmacokinetics and toxicity properties of silichristin and generate analogues

Molecule	GI absorption	BBB permeant	P-gp substrate	CYP inhibitor					Log K_p Cm/s	LD_{50} mol/kg
				1A2	2C19	2C9	2D6	3A4		
SIL1	Low	No	No	No	No	No	No	No	-8.06	2.883
SIL2	Low	No	No	No	No	No	No	No	-8.43	2.988
SIL3	Low	No	No	No	No	No	No	No	8.11	2.875
SIL4	Low	No	No	No	No	No	No	No	-8.06	2.872
SIL5	Low	No	No	No	No	No	No	No	-8.27	2.876
SIL6	Low	No	No	No	No	No	No	No	-8.65	2.892
SIL7	Low	No	No	No	No	No	No	No	-8.11	2.902
SIL8	Low	No	No	No	No	No	No	No	-8.11	2.882
SIL9	Low	No	No	No	No	No	No	No	-8.43	2.886
SIL10	Low	No	No	No	No	No	No	No	-8.27	2.883
SIL11	Low	No	No	No	No	No	No	No	-8.06	2.893
SIL12	Low	No	No	No	No	No	No	No	-8.81	2.828
SIL13	Low	No	No	No	No	No	No	No	-8.27	2.949
SIL14	Low	No	No	No	No	No	No	No	-8.06	2.875
SIL15	Low	No	No	No	No	No	No	No	-8.65	2.831
SIL16	Low	No	No	No	No	No	No	No	-8.27	2.910
SIL17	Low	No	No	No	No	No	No	No	-8.48	2.831
SIL18	Low	No	No	No	No	No	No	No	-8.81	2.830
SIL19	Low	No	No	No	No	No	No	No	-8.22	2.883
SIL20	Low	No	No	No	No	No	No	No	-8.11	2.808
Silichristin	Low	No	No	No	No	No	No	Yes	-8.14	2.614

Table 3. IC50 values of silichristin and selected derivatives against HPPD and AChE enzymes

Molecule	HPPD	AChE
	IC_{50} (µM)	IC_{50} (µM)
SIL1	1.80	3.55
SIL2	6.03	2.53
SIL3	2.53	**0.65**
SIL4	2.53	3.55
SIL5	2.99	2.99
SIL6	5.90	6.99
SIL7	**1.28**	1.28
SIL8	1.52	1.53
SIL9	2.53	6.99
SIL10	2.53	1.80
SIL11	2.53	2.53
SIL12	8.28	9.81
SIL13	1.80	0.91
SIL14	2.13	2.13

SIL15	4.18	4.20
SIL16	2.13	1.80
SIL17	2.53	2.53
SIL18	4.22	4.98
SIL19	3.55	3.55
SIL20	2.13	1.28
Silichristin	0.91	1.52

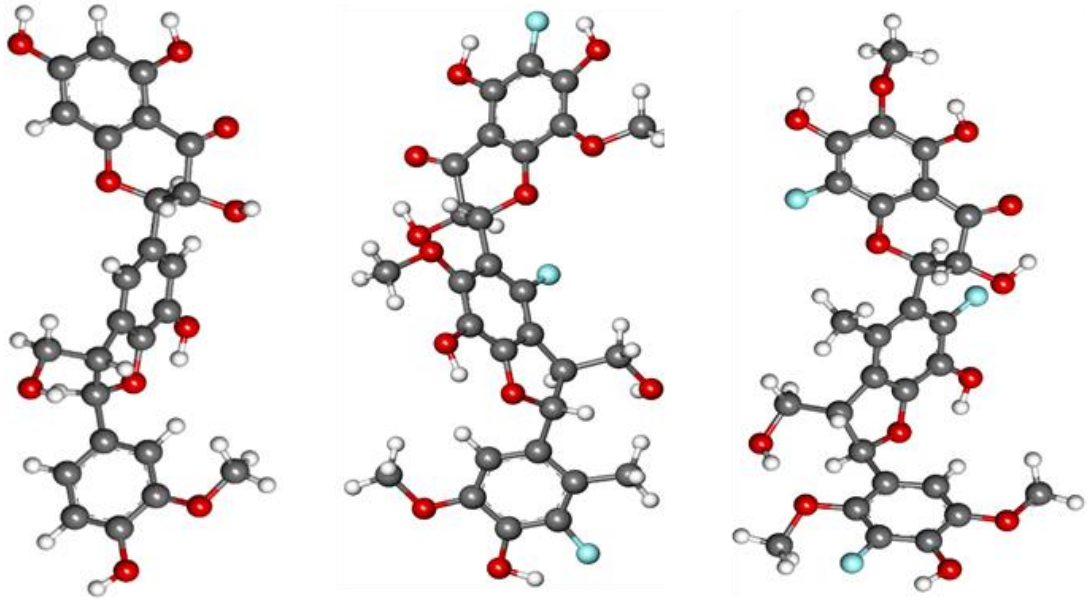

(a) (b) (c)

Figure 2. The optimized 3D-structure of Silichristin (a), SIL3 (b), and SIL7 (c) at DFT/B3LYP method

Following the prediction of pharmacokinetics-toxicity properties, the half maximal inhibitory concentration (IC50) of all the selected compounds against HPPD and AChE enzymes was calculated using AutoDock 4.2 and AutoDock Tools 1.5.6 software [36,37]. The obtained data are presented in Table 3.

Based on the in silico analysis of half maximal inhibitory concentration (IC_{50}) values provided in Table 3, SIL3 emerges as the most potent compound with the lowest IC_{50} value of 0.65 µM, suggesting its efficacy as an insecticide. Additionally, the data in Table 3 reveal SIL7 as the most potent compound acting as an herbicide. These findings highlight SIL3 and SIL7 as promising candidates, warranting further investigation through molecular docking and molecular dynamics analyses.

3.2. Computational perspective

3.2.1. Geometry optimization

Obtaining the optimized structure of small molecules is very crucial for elucidating their exact binding behavior. Therefore, to comprehensively understand this behavior, the structures of the highly potent compounds SIL3 and SIL7, along with Silichristin, were fully optimized using the DFT/B3LYP method as outlined in section 2.3. The resulting optimized ground state geometries of these compounds are depicted in Figure 2.

3.2.2. Molecular electrostatic potential surface and atomic charge

The molecular electrostatic potential (MEP) maps can be utilized to determine the regions of the reaction by specifying the distribution of electronic charges around the molecule. In the MEP surface, the blue color is relevant to the electron-deficient regions that are proper for the nucleophilic attack, and the red color is related to the electron-rich sites (proper for electrophilic attack) [36]. The green color represents neutral electrostatic potential sites. The 3D map of MEP was obtained for Silichristin, SIL3, and SIL7 by the same level of theory that was used for geometry optimization and is presented in

Figure 3. In these three compounds, the hydroxyl groups (red site) are more susceptible to electrophilic attack due to the higher negative charge surrounding this site. The green areas in these compounds indicate the neutral electrostatic potential. The MEP value of Silichristin, SIL3, and SIL7 ranged from –
1.7 to +1.7, -1.6 to +1.6, and -2.0 to +2.0, respectively.

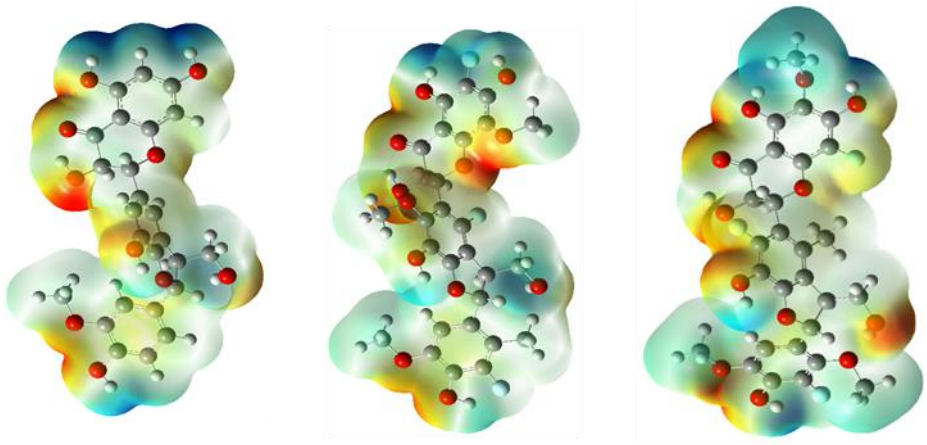

(a) (b) (c)

Figure 3. Molecular electrostatic potential representation for Silichristin (a), SIL3 (b), and SIL7 (c) at DFT/B3LYP method

3.2.3. HOMO-LUMO analysis

The interplay between HOMO-LUMO surfaces plays a crucial role in governing molecular interactions, offering valuable insights into the chemical behavior and reactivity of compounds [37]. Defined as the energy gap between the HOMO and LUMO orbitals ($\Delta E = E_{LUMO} - E_{HOMO}$), this parameter is pivotal in understanding intramolecular charge transfer interactions.

The HOMO, serving as the electron donor orbital, and the LUMO, acting as the electron acceptor orbital, are named so due to their respective states of electron occupancy, the HOMO is filled with electrons, while the LUMO is devoid of them. Employing the B3LYP/6-311G++(d,p) method, we computed the HOMO-LUMO energy surfaces of the compounds Silichristin, SIL3, and SIL7, as illustrated in Figure 4. In the case of Silichristin and Sil7, the HOMO orbital predominantly localizes on the phenyl-tetrahydropyran and phenyl-dihydrofuran parts. Conversely, in SIL3, the HOMO orbitals shift towards the tetrahydronaphthalene and phenyl-tetrahydropyran parts. However, the LUMO orbitals are consistently situated on the tetrahydronaphthalene for all three compounds.

The magnitude of the HOMO-LUMO energy gap provides critical insights into the chemical reactivity of a compound [38]. Smaller ΔE values indicate higher chemical reactivity. Conversely, a larger energy gap signifies lower chemical reactivity [39,40].

According to the data depicted in Figure 4, the ground state energies of HOMO and LUMO for Silichristin are -3.00 and -0.93 eV, respectively, resulting in a calculated ΔE of 3.94 eV. For SIL3 and SIL7, the HOMO and LUMO energies are -2.96, 0.97 eV and -5.62, -1.64 eV, respectively, with ΔE values of 3.93 and 3.98 eV, respectively. Based on the obtained data, the order of increasing chemical reactivity is as follows: SIL3 > Silichristin > SIL7. This order of reactivity stands in good agreement with the same order of the predicted IC_{50} values for the three compounds.

3.2.4. Molecular docking study

To elucidate the mode of interaction between the most potent silichristin analogues and the receptors HPPD and AChE, molecular docking simulations were conducted. These simulations aim to predict the most stable conformation of the most potent silichristin analogues when bound to the selected target receptors HPPD and AChE. In our study, multiple docking runs were performed, revealing the optimal binding poses for SIL3, SIL7, and Silichristin in complex with HPPD and AChE, as depicted in Figure 5. Additionally, Figure 5 illustrates that hydrogen bonding is the predominant mode of interaction.

The obtained binding free energies, reacting residues, and H-bonds length for SIL3, SIL7, and Silichristin are detailed in Table 5. Our results indicate that SIL3 exhibits the strongest binding affinity towards AChE, followed by Silichristin with HPPD, SIL7 with AChE, and Silichristin with HPPD. This highlights the robust interaction between SIL3, SIL7, and Silichristin with the HPPD and AChE receptors.

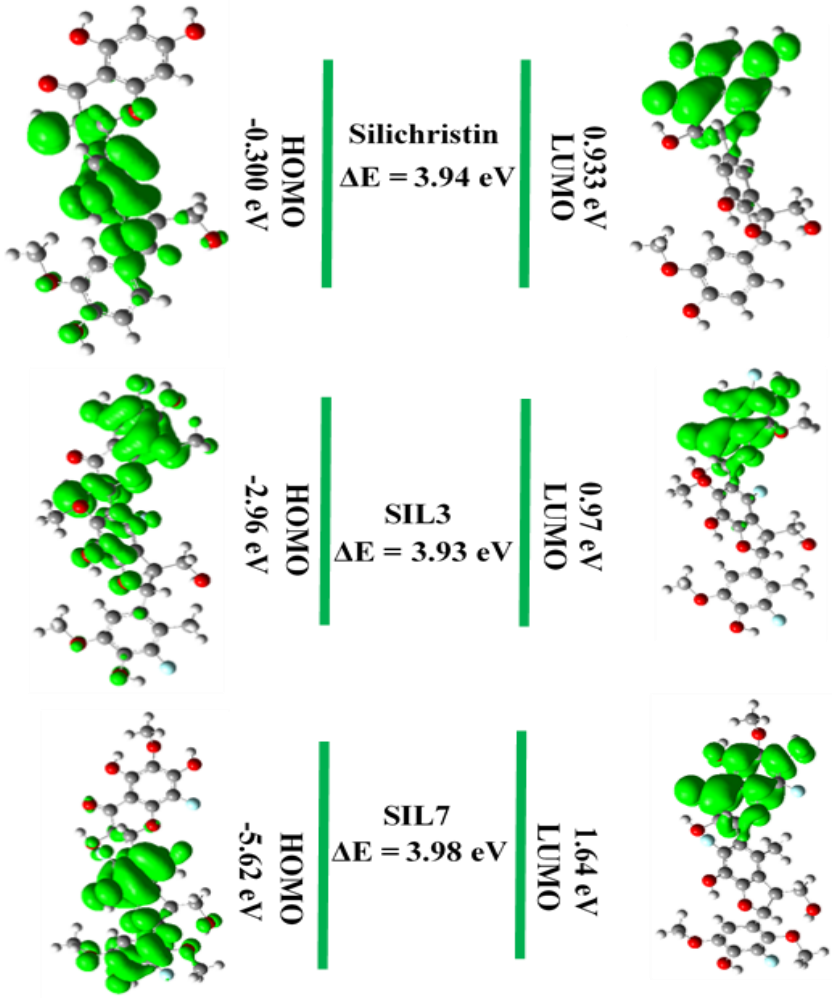

Figure 4. HOMO-LUMO diagram of Silichristin (a), SIL3 (b), and SIL7 (c) estimated by DFT/B3LYP approach

3.2.5. Molecular Dynamic simulation

Molecular dynamics simulations for a duration of 100 ns were conducted for the SIL3, SIL7, and Silichristin. The objective was to observe their interaction patterns and stability at the binding sites of HPPD and AChE. The dynamic behavior of the entire simulated system was thoroughly analyzed using parameters such as Root Mean Square Deviation (RMSD), Root Mean Square Fluctuation (RMSF), and radius of gyration.

3.2.5.1. Root mean square deviation (RMSD)

To assess the stability of the protein-ligand complexes formed with SIL3, SIL7, and Silichristin, the RMSD of carbon alpha atoms was calculated from the simulation trajectories [41,42], (Figure 6). Following equilibration, the RMSD values of both complexes remained stable in the range of approximately 1.5-2 Å. Subsequently, the RMSD of the SIL3 complex increased to 3 Å and maintained this level until the end of the simulation. Conversely, the RMSD values of the SIL7 complex did not exhibit significant deviations throughout the simulation. The consistent RMSD values indicate the stability of the protein-ligand complexes.

3.2.5.2. Root mean square fluctuation (RMSF)

To evaluate the dynamic behavior of the protein when bound to the ligands, we calculated the root mean square fluctuations (RMSF) values. These

values provide insights into the flexibility and movement of individual protein residues throughout the entire simulation duration [43]. Upon analyzing the RMSF values, we observed that the majority of protein residues exhibited minimal fluctuations, measuring less than 2 Å, throughout the simulation. This suggests that these residues maintained a relatively rigid and stable conformation in the presence of the ligands. However, the loop regions of the protein demonstrated higher RMSF values, peaking at approximately 9 Å (Figure 7). The RMSF analysis indicates that the protein-ligand complex remained stable overall, with most residues adopting a rigid conformation. The elevated RMSF values observed in the loop regions suggest that these areas experienced more pronounced fluctuations and potentially engaged in dynamic interactions with the ligands. In summary, the RMSF values support the notion of a stable protein-ligand complex, as the majority of protein residues displayed minimal fluctuations, while the loop regions exhibited relatively higher flexibility.

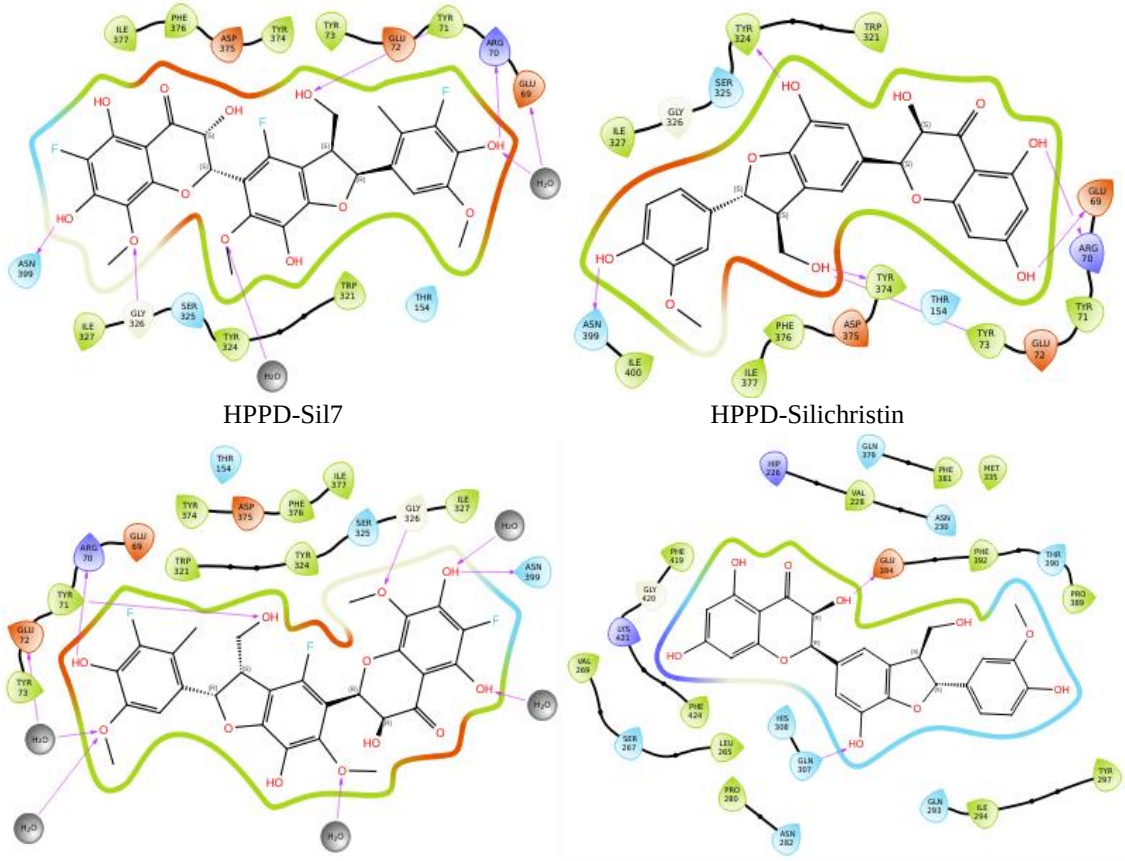

HPPD-Sil7 HPPD-Silichristin

AChE-SIL3 AChE-Silichristin

Figure 5. 3D interaction between the most potent Silichristin analogues and the targets HPPD and AChE where the redlines represent the H-bonds

Table 5. Molecular docking and bond interactions analysis of Silichristin, SIL3, and SIL7 candidates with the receptors (HPPD) and AChE

Acetylcholinesterase (AChE) (ID: 6xyu)			
Ligand code	Center grid box x, y, z	H-bond (Reacting residues distance Å)	Binding energy (kcal/mol)
SIL3	33.05, 67.37, 09.81	ARG70 (1.83), TYR71 (1.84), GLY326 (1.98), ASN399 (1.82)	-8.4
Silichristin	30.3 -22.9, 04.6	GLN307 (2.56), GLU394 (1.48)	-7.9
4-hydroxyphenylpyruvate dioxygenase (HPPD) (ID: 6J63)			
SIL7	41.3, 60.4, 03.8	ARG70 (1.72), GLU72 (1.83), ASN399 (1.90), GLY326 (2.10)	-8.1
Silichristin	33.0, 67.4, 09.80	GLU69 (1.92), ARG70 (2.07), TYR324 (2. 53), ASN399 (2.26), TYR374 (2.15),	-8.2

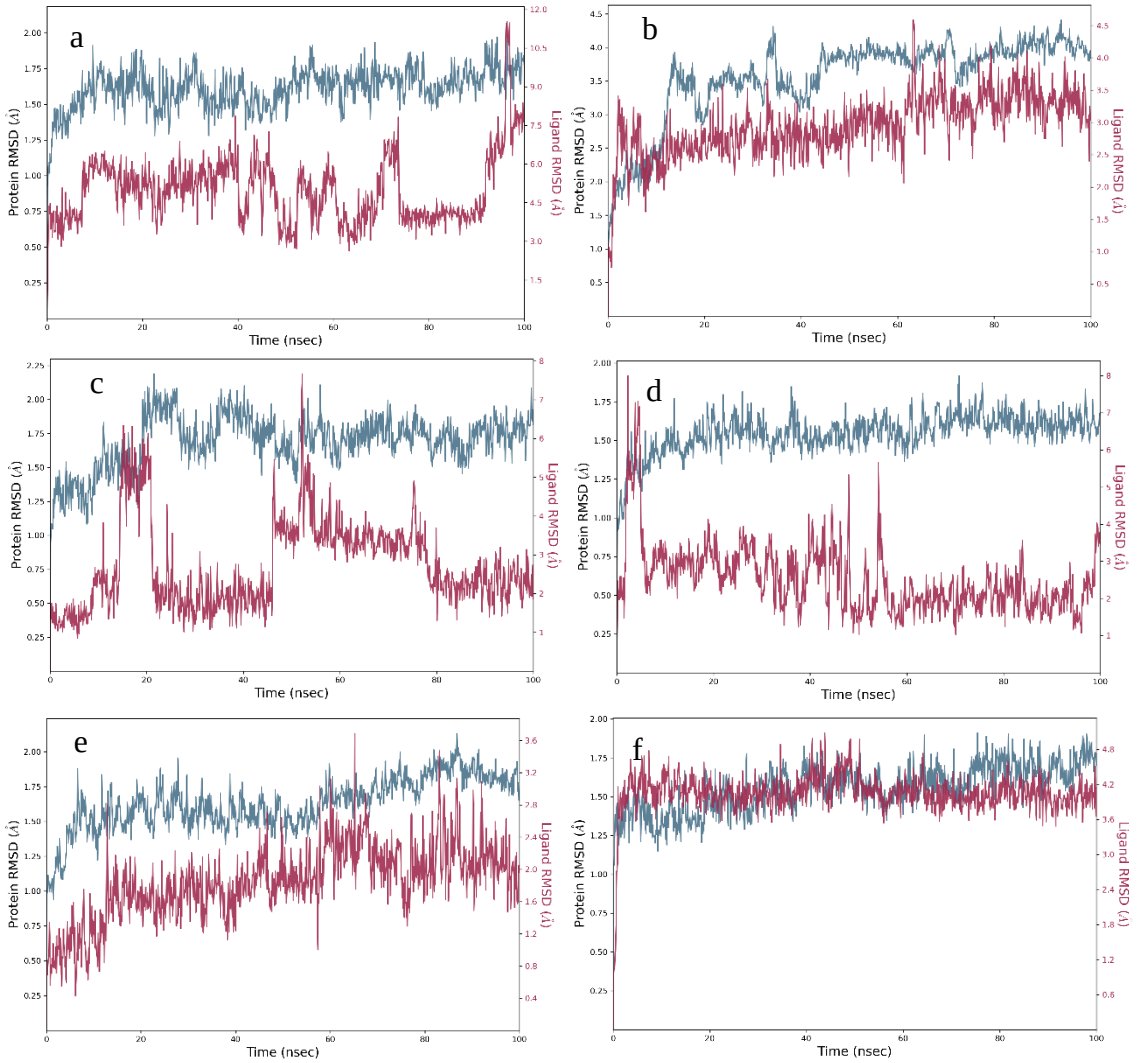

Figure 6. The RMSD plots of HPPD and AChE complexes during 100 ns simulation (a) Silichristin-AChE, (b) Silichristin-HPPD, (c) SIL3-AChE, (d) SIL3-HPPD (e) SIL7-AChE, SIL7-HPPD (f)

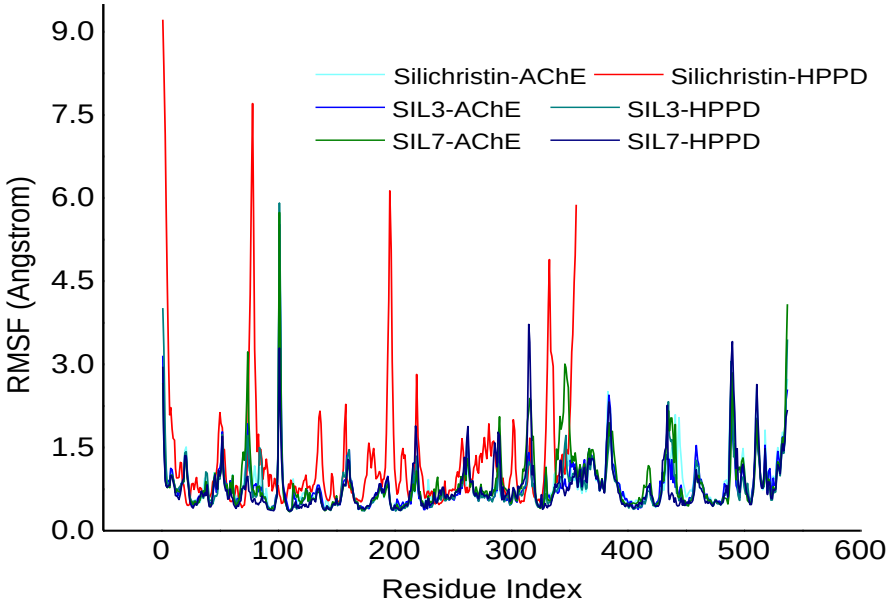

Figure 7. The fluctuation of protein residues during simulations as determined by RSMF values

3.2.5.3. Radius of gyration (Rg)

To evaluate the structural compactness of the AChE and HPPD proteins in complex with the compounds Silichristin, SIL3, and SIL7, we conducted an analysis of the radius of gyration (Rg). The Rg values provide insights into the overall compactness of the protein structure, where lower values indicate a more compact structure and higher values suggest unfolding events during the simulation [44]. The Rg plots of the protein-ligand complexes revealed that the Rg values remained stable within the range of 6.03 to 5.17 Å throughout the simulation, Figure 8. This indicates that the enzyme structure maintained its compacted conformation when bound to Silichristin, SIL3, and SIL7 compounds. The consistent Rg values further support the notion of structural stability during the simulation period.

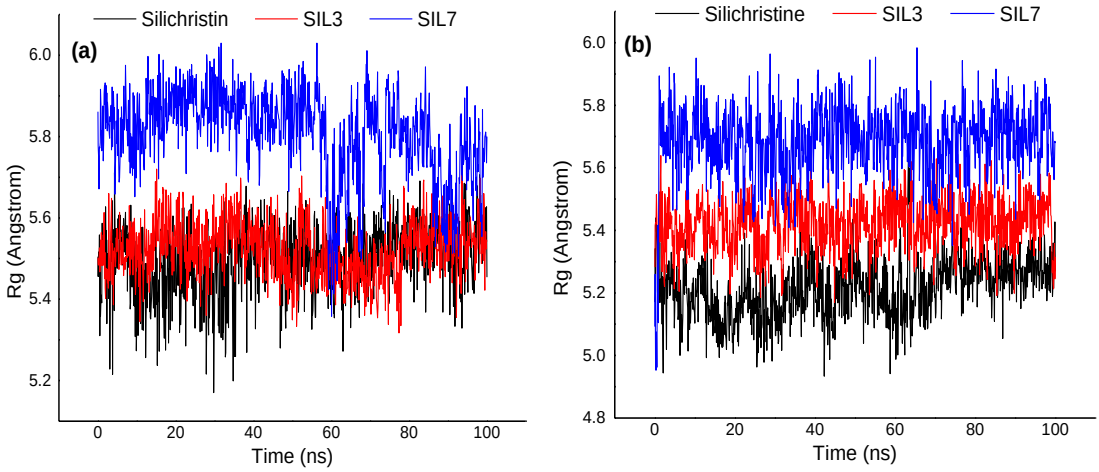

Figure 8. The Rg plots of AChE-Silichristin, AChE-SIL3, AChE-SIL7 (a) and HPPD-Silichristin, HPPD-SIL3, HPPD-SIL7 (b) complexes as a function of simulation time.

4. Conclusions

This in silico assessment has provided valuable insights into the pesticidal potential of silichristin analogues derived from *Silybum marianum*. Through virtual screening, molecular docking, and molecular dynamics simulations, we have elucidated the pharmacokinetic-toxicity properties and molecular interactions of these compounds, shedding light on their suitability as novel pesticides.

Our findings reveal that the silichristin analogues exhibit activity against key pesticide targets, including 4-hydroxyphenylpyruvate dioxygenase (HPPD) and acetylcholinesterase (AChE) receptors. Specifically, compounds SIL3 and SIL7 demonstrated strong binding affinities with the target proteins, indicating their potential efficacy as pesticides. Moreover, molecular dynamics simulations confirmed the stability of the protein-ligand complexes over extended periods, suggesting sustained activity of the compounds within the biological systems.

Importantly, our study highlights the importance of utilizing computational approaches in pesticide discovery and development. By leveraging in silico methodologies, we can efficiently screen large compound libraries, prioritize candidates based on their pharmacological profiles, and gain mechanistic insights into their mode of action. This accelerates the pesticide discovery process and reduces reliance on conventional trial-and-error approaches, thereby facilitating the identification of safer and more environmentally friendly pest control agents.

Moving forward, our findings pave the way for further experimental validation of the identified silichristin analogues as potential pesticides.

References

[1] C.R. de Avelar, E.M. Pereira, P.R. de Farias Costa, R.P. de Jesus, L.P.M. de Oliveira, Effect of silymarin on biochemical indicators in patients with liver disease: Systematic review with meta-analysis, World J Gastroenterol 23 (2017) 5004.

[2] L. Grădinariu, L. Dediu, M. Crețu, I.R. Grecu, A. Docan, D.I. Istrati, F.M. Dima, M.D. Stroe, C. Vizireanu, The Antioxidant and Hepatoprotective Potential of Berberine and Silymarin on Acetaminophen Induced

Toxicity in Cyprinus carpio L., Animals 14 (2024) 373.

[3] F. Angelico, Chronic liver disease and management with silymarin: an introductory review of a clinical case collection, Drugs Context 13 (2024) 1–9.

[4] H.M. Jaffar, F. Al-Asmari, F.A. Khan, M.A. Rahim, E. Zongo, Silymarin: Unveiling its pharmacological spectrum and therapeutic potential in liver diseases—A comprehensive narrative review, Food Sci Nutr (2024) 3097-3111.

[5] C.E. Kazazis, A.A. Evangelopoulos, A. Kollas, N.G. Vallianou, The Therapeutic Potential of Milk Thistle in Diabetes, The Review of Diabetic Studies 11 (2014) 167–174.

[6] W. Borymska, M. Zych, S. Dudek, I. Kaczmarczyk-Sedlak, Silymarin from Milk Thistle Fruits Counteracts Selected Pathological Changes in the Lenses of Type 1 Diabetic Rats, Nutrients 14 (2022) 1450.

[7] A. Doostkam, M. Fathalipour, M.H. Anbardar, A. Purkhosrow, H. Mirkhani, Therapeutic Effects of Milk Thistle (Silybum marianum L.) and Artichoke (Cynara scolymus L.) on Nonalcoholic Fatty Liver Disease in Type 2 Diabetic Rats, Can J Gastroenterol Hepatol 2022 (2022) 1–8.

[8] O. Porwal, M.S. Mohammed Ameen, E.T. Anwer, S. Uthirapathy, J. Ahamad, A. Tahsin, Silybum marianum (Milk Thistle): Review on Its chemistry, morphology, ethno medical uses, phytochemistry and pharmacological activities, Journal of Drug Delivery and Therapeutics 9 (2019) 199–206.

[9] S. Sultana, M. Asaduzzaman, Allelopathic Studies on Milk Thistle (Silybum marianum), International Journal of Agricultural Research, Innovation and Technology 2 (2013) 62–67.

[10] M.N. Akhtar, R. Saeed, F. Saeed, A. Asghar, S. Ghani, H. Ateeq, A. Ahmed, A. Rasheed, M. Afzaal, M. Waheed, B. Hussain, M. Asif Shah, Silymarin: a review on paving the way towards promising pharmacological agent, Int J Food Prop 26 (2023) 2256–2272.

[11] M. Bijak, Silybin, a Major Bioactive Component of Milk Thistle (Silybum marianum L. Gaernt.)—Chemistry, Bioavailability, and Metabolism, Molecules 22 (2017) 1942.

[12] C.S. Chambers, V. Holečková, L. Petrásková, D. Biedermann, K. Valentová, M. Buchta, V. Křen, The silymarin composition… and why does it matter???, Food Research International 100 (2017) 339–353. https://doi.org/10.1016/j.foodres.2017.07.017.

[13] A. Santucci, G. Bernardini, D. Braconi, E. Petricci, F. Manetti, 4-Hydroxyphenylpyruvate Dioxygenase and Its Inhibition in Plants and Animals: Small Molecules as Herbicides and Agents for the Treatment of Human Inherited Diseases, J Med Chem 60 (2017) 4101–4125. https://doi.org/10.1021/acs.jmedchem.6b01395.

[14] S.E. McComic, S.O. Duke, E.R. Burgess, D.R. Swale, Defining the toxicological profile of 4-hydroxyphenylpyruvate dioxygenase-directed herbicides to Aedes aegypti and Amblyomma americanum, Pestic Biochem Physiol 194 (2023) 105532.

[15] M.B. Colovic, D.Z. Krstic, T.D. Lazarevic-Pasti, A.M. Bondzic, V.M. Vasic, Acetylcholinesterase Inhibitors: Pharmacology and Toxicology, Curr Neuropharmacol 11 (2013) 315–335.

[16] Y.H. Kim, J.Y. Choi, Y.H. Je, Y.H. Koh, S.H. Lee, Functional analysis and molecular characterization of two acetylcholinesterases from the German cockroach, *Blattella germanica*, Insect Mol Biol 19 (2010) 765–776.

[17] A.M. Dos Santos, A.C. Moreira, B.R. Lopes, M.F. Fracola, F.G. de Almeida, O.C. Bueno, Q.B. Cass, D.H.F. Souza, Acetylcholinesterases from Leaf-Cutting ant *Atta sexdens* : Purification, Characterization, and Capillary Reactors for On-Flow Assays, Enzyme Res 2019 (2019) 1–9.

[18] S. Thapa, M. Lv, H. Xu, Acetylcholinesterase: A Primary Target for Drugs and Insecticides, Mini-Reviews in Medicinal Chemistry 17 (2017).

[19] G.-J. Lang, K. Yan Zhu, C.-X. Zhang, Can Acetylcholinesterase Serve as a Target for Developing More Selective Insecticides? Curr Drug Targets 13 (2012) 495–501.

[20] P. Zhang, C.-B. Duan, B. Jin, A.S. Ali, X. Han, H. Zhang, M.-Z. Zhang, W.-H. Zhang, Y.-C. Gu, Recent advances in the natural products-based lead discovery for new agrochemicals, Advanced Agrochem 2 (2023) 324–339.

[21] B. Verma, H. Karakoti, R. Kumar, S.K. Mahawer, O. Prakash, R.M. Srivastava, S. Kumar, S. Rawat, D.S. Rawat, M.S. de Oliveira, Phytochemical Screening and Evaluation of Pesticidal Efficacy in the Oleoresins of Globba sessiliflora Sims and In Silico Study, Evidence-Based Complementary and Alternative Medicine 2023 (2023) 1–16.

[22] J.E. Casida, G.B. Quistad, Why Insecticides are More Toxic to Insects than People: The Unique Toxicology of Insects, J Pestic Sci 29 (2004) 81–86.

[23] A. Speck-Planche, V. V. Kleandrova, M.T. Scotti, Fragment-based approach for the in silico discovery of multi-target insecticides, Chemometrics and Intelligent Laboratory Systems 111 (2012) 39–45.

[24] S.-H. Lee, K.B. Ha, D.H. Park, Y. Fang, J.H. Kim, M.G. Park, R.M. Woo, W.J. Kim, I.-K. Park, J.Y. Choi, Y.H. Je, Plant-derived compounds regulate formation of the insect juvenile hormone receptor complex, Pestic Biochem Physiol 150 (2018) 27–32.

[25] M. Jankowska, J. Rogalska, J. Wyszkowska, M. Stankiewicz, Molecular Targets for Components of Essential Oils in the Insect Nervous System—A Review, Molecules 23 (2017) 34.

[26] A. Schüller, V. Hähnke, G. Schneider, SmiLib v2.0: A Java-Based Tool for Rapid Combinatorial Library Enumeration, QSAR Comb Sci 26 (2007) 407–410.

[27] A. Daina, O. Michielin, V. Zoete, SwissADME: a free web tool to evaluate pharmacokinetics, drug-likeness and medicinal chemistry friendliness of small molecules, Scientific Reports 2017 7:1 7 (2017) 1–13.

[28] D.E. V. Pires, T.L. Blundell, D.B. Ascher, pkCSM: Predicting Small-Molecule Pharmacokinetic and Toxicity Properties Using Graph-Based Signatures, J Med Chem 58 (2015) 4066–4072.

[29] M. Frisch, G. Trucks, H. Schlegel, G.S.-Wallingford, U. CT, U. 2009, Gaussian 16; Gaussian, Inc, Gaussian, (2016).

[30] S. Kim, J. Chen, T. Cheng, A. Gindulyte, J. He, S. He, Q. Li, B.A. Shoemaker, P.A. Thiessen, B. Yu, L. Zaslavsky, J. Zhang, E.E. Bolton, PubChem 2023 update, Nucleic Acids Res 51 (2023) D1373–D1380.

[31] H. Lin, J. Yang, D. Wang, G. Hao, J. Dong, Y. Wang, W. Yang, J. Wu, C. Zhan, G. Yang, Molecular insights into the mechanism of 4-hydroxyphenylpyruvate dioxygenase inhibition: enzyme kinetics, X-ray crystallography and computational simulations, FEBS J 286 (2019) 975–990.

[32] F. Nachon, T.L. Rosenberry, I. Silman, J.L. Sussman, A Second Look at the Crystal Structures of Drosophila melanogaster Acetylcholinesterase in Complex with Tacrine Derivatives Provides Insights Concerning Catalytic Intermediates and the Design of Specific Insecticides, Molecules 25 (2020) 1198.

[33] H.M. Berman, T. Battistuz, T.N. Bhat, W.F. Bluhm, P.E. Bourne, K. Burkhardt, Z. Feng, G.L. Gilliland, L. Iype, S. Jain, P. Fagan, J. Marvin, D. Padilla, V. Ravichandran, B. Schneider, N. Thanki, H. Weissig, J.D. Westbrook, C. Zardecki, The Protein Data Bank, Acta Crystallogr D Biol Crystallogr 58 (2002) 899–907.

[34] Schrödinger Release 2023-4: Maestro, Schrödinger, LLC, New York, NY, 2023, (n.d.).

[35] R.A. Friesner, R.B. Murphy, M.P. Repasky, L.L. Frye, J.R. Greenwood, T.A. Halgren, P.C. Sanschagrin, D.T. Mainz, Extra Precision Glide: Docking and Scoring Incorporating a Model of Hydrophobic Enclosure for Protein−Ligand Complexes, J Med Chem 49 (2006) 6177–6196.

[36] M. Feizi-Dehnayebi, E. Dehghanian, H. Mansouri-Torshizi, DNA/BSA binding affinity studies of new Pd(II) complex with S-S and N-N donor mixed ligands via experimental insight and molecular simulation: Preliminary antitumor activity, lipophilicity and DFT perspective, J Mol Liq 344 (2021) 117853.

[37] S. Sevvanthi, S. Muthu, M. Raja, Molecular docking, vibrational spectroscopy studies of (RS)-2-(tert-butylamino)-1-(3-

chlorophenyl)propan-1-one: A potential adrenaline uptake inhibitor, J Mol Struct 1173 (2018) 251–260.

[38] K. Karrouchi, S.A. Brandán, Y. Sert, H. El-marzouqi, S. Radi, M. Ferbinteanu, M.E.A. Faouzi, Y. Garcia, M. Ansar, Synthesis, X-ray structure, vibrational spectroscopy, DFT, biological evaluation and molecular docking studies of (E)-N'-(4-(dimethylamino)benzylidene)-5-methyl-1H-pyrazole-3-carbohydrazide, J Mol Struct 1219 (2020) 128541.

[39] M. Alizadeh, Z. Mirjafary, H. Saeidian, Straightforward synthesis, spectroscopic characterizations and comprehensive DFT calculations of novel 1-ester 4-sulfonamide-1,2,3-triazole scaffolds, J Mol Struct 1203 (2020) 127405.

[40] K. Karrouchi, S.A. Brandán, Y. Sert, H. El-marzouqi, S. Radi, M. Ferbinteanu, M.E.A. Faouzi, Y. Garcia, M. Ansar, Synthesis, X-ray structure, vibrational spectroscopy, DFT, biological evaluation and molecular docking studies of (E)-N'-(4-(dimethylamino)benzylidene)-5-methyl-1H-pyrazole-3-carbohydrazide, J Mol Struct 1219 (2020) 128541.

[41] M.F. AlAjmi, M.T. Rehman, A. Hussain, Celecoxib, Glipizide, Lapatinib, and Sitagliptin as potential suspects of aggravating SARS-CoV-2 (COVID-19) infection: a computational approach, J Biomol Struct Dyn 40 (2022) 13747–13758.

[42] P. Taslimi, Y. Erden, S. Mamedov, L. Zeynalova, N. Ladokhina, R. Tas, B. Tuzun, A. Sujayev, N. Sadeghian, S.H. Alwasel, I. Gulcin, The biological activities, molecular docking studies, and anticancer effects of 1-arylsuphonylpyrazole derivatives, J Biomol Struct Dyn (2020) 1–11.

[43] D. Iqbal, M.T. Rehman, A. Bin Dukhyil, S.M.D. Rizvi, M.F. Al Ajmi, B.M. Alshehri, S. Banawas, M.S. Khan, W. Alturaiki, M. Alsaweed, High-Throughput Screening and Molecular Dynamics Simulation of Natural Product-like Compounds against Alzheimer's Disease through Multitarget Approach, Pharmaceuticals 14 (2021) 937.

[44] Md.T. Rehman, M.F. AlAjmi, A. Hussain, Natural Compounds as Inhibitors of SARS-CoV-2 Main Protease (3CLpro): A Molecular Docking and Simulation Approach to Combat COVID-19, Curr Pharm Des 27 (2021) 3577–3589.